

RESEARCH

Open Access



Bogdanov–Takens bifurcation of a Holling IV prey–predator model with constant-effort harvesting

Lifang Cheng^{1*} and Litao Zhang^{1,2}

*Correspondence: lfczam@126.com

¹School of Mathematics,
Zhengzhou University of
Aeronautics, Zhengzhou, Henan
450046, P.R. China
Full list of author information is
available at the end of the article

Abstract

A prey–predator model with constant-effort harvesting on the prey and predators is investigated in this paper. First, we discuss the number and type of the equilibria by analyzing the equations of equilibria and the distribution of eigenvalues. Second, with the rescaled harvesting efforts as bifurcation parameters, a subcritical Hopf bifurcation is exhibited near the multiple focus and a Bogdanov–Takens bifurcation is also displayed near the BT singularity by analyzing the versal unfolding of the model. With the variation of bifurcation parameters, the system shows multi-stable structure, and the attractive domains for different attractors are constituted by the stable and unstable manifolds of saddles and the limit cycles bifurcated from Hopf and Bogdanov–Takens bifurcations. Finally, a cusp point and two generalized Hopf points are found on the saddle-node bifurcation curve and the Hopf bifurcation curves, respectively. Several phase diagrams for parameters near one of the generalized Hopf points are exhibited through the generalized Hopf bifurcation.

MSC: 34C23; 34D20; 37G15; 37G10

Keywords: Hopf bifurcation; Bogdanov–Takens bifurcation; Lyapunov number; Cusp bifurcation; Generalized Hopf bifurcation

1 Introduction

The prey–predator model based on Lotka–Volterra model is one of the most popular models in mathematical ecology and has been widely applied in understanding population dynamics of the species, which is characterized by the complicated interaction among the species and the interaction between the species and their surroundings. Functional response is the rate of prey consumption by the predators, which can characterize the interaction between the prey and the predators. The initial functional responses are presented by Holling in [11, 12] and have been classified into three types called Holling I, II and III. Generally speaking, Holling type I response is seen mostly at filter-feeding predators, such as mollusks, algae, and cells. Holling types II and III responses are applicable to the invertebrates and complicated vertebrates, respectively. The common feature of these functions is all monotonic increasing and bounded, which means that the more the prey is in the environment, the better for the predators [6]. However, many experiments and observations

© The Author(s) 2021. This article is licensed under a Creative Commons Attribution 4.0 International License, which permits use, sharing, adaptation, distribution and reproduction in any medium or format, as long as you give appropriate credit to the original author(s) and the source, provide a link to the Creative Commons licence, and indicate if changes were made. The images or other third party material in this article are included in the article's Creative Commons licence, unless indicated otherwise in a credit line to the material. If material is not included in the article's Creative Commons licence and your intended use is not permitted by statutory regulation or exceeds the permitted use, you will need to obtain permission directly from the copyright holder. To view a copy of this licence, visit <http://creativecommons.org/licenses/by/4.0/>.

indicate that monotonicity does not always hold and a non-monotonic response may exist when the nutrient concentration reaches a high level [3, 9, 31]. It is also explained that when the number of the prey is large enough, their group defense ability and camouflage ability are strengthened to decrease the predation ability of the predators. For example, large swarms of insects make individual identification difficult for their predators. A lone musk ox can be successfully attacked by wolves, while large groups of musk oxen are less likely to be attacked successfully [28]. Filamentous algae are often qualified as inedible by herbivorous zooplankton [8]. To model such an inhibitory effect, a Holling IV response $\frac{mx}{a+bx+x^2}$ and a simplified Holling IV response $\frac{mx}{a+x^2}$ have been proposed by Andrews [1] and Sokoland [25], respectively. Since then the prey–predator system with Holling IV functional response has been widely studied by many researchers [4, 15, 20, 30, 32].

For commercial and economical purposes, the exploitation of biological resources and harvesting of populations are commonly practiced in fishery, forestry and wildlife management [22]. It is known that harvesting, as a scientific management of renewable resources, has a strong effect on the dynamic evolution of the biological models, which can determine the survival and sustainable development of the species. In order to reasonably govern renewable resources, the study of the exploitation of biological resources and harvesting of populations is becoming a hot topic in the field of biological economics, which is related to the optimal management of renewable resources [5].

Recently, it has become very popular among many researchers in using bifurcation theory to analyze the harvested prey–predator model to reach an optimal management in the field of mathematical biology [10, 13, 15–18, 21, 29, 33, 34], which can predict the species’ evolutionary direction, including the constant state, periodic state and chaotic state, as the critical biological parameters vary.

From the present work, we find that most of the harvested prey–predator models which have been considered by many authors are confined to three aspects: (i) constant-yield harvesting, (ii) harvesting subjected to only one species or (iii) the numerical response is proportional to the functional response, where the numerical response is the change in predator density as a function of change in prey density [26]. It is the reproduction rate of a consumer as a function of food density. That is, when the predators consume their prey, the numerical response is dynamic relation between the increasing number of the predators and the consumed prey. From the convention, we know that harvesting frequently varies with season, market demand, the species quantity, harvesting cost and so on; the prey and the predators can be both valuable from the business point; the numerical response can be uncorrelated with the functional response. Based on above analysis and the virtue of the Holling IV response, in this paper we extend previous work from three aspects and establish a prey–predator model with Leslie–Gower and Holling IV schemes with constant-effort harvesting, which is given by

$$\begin{aligned} \dot{x} &= r_1x \left(1 - \frac{x}{K}\right) - \frac{mx}{b+x^2}y - c_1x, \\ \dot{y} &= r_2y \left(1 - \frac{y}{sx}\right) - c_2y. \end{aligned} \tag{1.1}$$

The logistic model $r_1x(1 - \frac{x}{K})$ is used to describe the growth of the prey in the absence of predators in the limited environmental carrying capacity. The second term $\frac{mx}{b+x^2}y$ describes

the change in the density of the prey attacked per unit time as the prey density changes. The last term c_1x is the constant-effort harvesting of the prey. $r_2y(1 - \frac{y}{sx})$ is the predator growth term, which is described by the Leslie–Gower function. $\frac{y}{sx}$ measures the loss in the predator population due to rarity (per capita of $\frac{y}{x}$) of its favorite term [19]. The term c_2y is the constant-effort harvesting of the predators. The meanings of the parameters are given as follows:

- (i) x and y denote the densities of the prey and the predators.
- (ii) K is the environmental carrying capacity for the prey.
- (iii) m denotes the maximal predation rate.
- (iv) b is the so-called half-saturation constant.
- (v) s is a measure of food quality that the prey provides for conversion into the predator birth.
- (vi) r_1 and r_2 are intrinsic growth rates of the prey and predators, respectively.
- (vii) c_1 and c_2 measure the effort being spent by a harvesting agency (harvesting efforts).

The model (1.1) without harvesting (i.e., $c_1 = c_2 = 0$) has been discussed in [7, 14, 20]. Li and Xiao [20] proved that the model could simultaneously undergo a Bogdanov–Takens bifurcation and a subcritical Hopf bifurcation in the small neighborhoods of two different equilibria, respectively. It was shown that for different parameters the model could have a stable limit cycle enclosing two equilibria, or an unstable limit cycle enclosing a hyperbolic equilibria, or two limit cycles enclosing a hyperbolic equilibrium. In Ref. [14], for the same model, Huang et al. investigated the degenerate Bogdanov–Takens bifurcation of codimension 3 around the degenerate positive equilibrium. Some other abundant dynamical phenomena could emerge, such as the coexistence of three hyperbolic positive equilibria, a homoclinic loop enclosing an unstable limit cycle, or a stable limit cycle enclosing three unstable hyperbolic positive equilibria. From the above-mentioned work, Hopf cyclicity and the global dynamics of the same model were investigated by Dai and Zhao [7] for the cases of one non-degenerate positive equilibrium and three distinct positive equilibria, respectively. Some explicit conditions for the globally stable equilibrium were established by applying Dulac’s criterion and constructing the Lyapunov function. It was shown that the Hopf bifurcation could occur at each weak focus and more complicated and new dynamics were observed. When the system had a unique positive equilibrium, there existed parameter values such that the system had two limit cycles around it. When the system had three positive equilibria, one limit cycle could bifurcate from each of the two positive anti-saddles simultaneously.

In order to discuss if the added harvesting terms can affect the bifurcation structure of the prey–predator model, we also do a series of bifurcation analysis for the model with linear harvesting. We find that, besides some original dynamical behaviors, some new phenomena and bifurcations appear in the harvested model, such as a globally stable equilibrium, a cusp bifurcation and a generalized Hopf bifurcation. From the cusp point, two saddle-node bifurcation curves are bifurcated, through which three equilibria collide to form an equilibrium or one equilibrium splits into three equilibria. From the generalized Hopf bifurcation point, a fold bifurcation curve of limit cycles is bifurcated, on which two limit cycles with different stability collide to form a semi-stable cycle. These dynamical behaviors have not been found or discussed in the original model in Ref. [7, 14, 20].

Before entering the topic, we carry out the following scaling transformations:

$$\begin{aligned} \bar{t} &= r_1 t, & \bar{x} &= \frac{x}{K}, & \bar{y} &= \frac{my}{r_1 K^2}, & a &= \frac{b}{K^2}, & \delta &= \frac{r_2}{r_1}, & \beta &= \frac{r_2 K}{sm}, \\ h_1 &= \frac{c_1}{r_1}, & h_2 &= \frac{c_2}{r_2}. \end{aligned}$$

Dropping the bars system (1.1) becomes

$$\begin{aligned} \dot{x} &= x(1-x) - \frac{x}{a+x^2}y - h_1x, \\ \dot{y} &= y\left(\delta - \beta\frac{y}{x}\right) - h_2y, \end{aligned} \tag{1.2}$$

where a, δ, β, h_1 and h_2 are positive parameters. h_1 and h_2 are called rescaled harvesting efforts. From the perspective of biology, system (1.2) is defined on the set $D = \{(x, y) \in \mathbb{R}^2 | x > 0, y \geq 0\}$.

By analyzing (1.2), we can prove that solution trajectories starting from the initial value $(x_0, 0)$ remain within the positive x -axis for all the time. Through integrating two equations in (1.2) and discussing the initial value $x(0) > 1 - h_1$ or $x(0) < 1 - h_1$, we can get the following lemma (the detailed proof is similar to Appendix A in [24]).

Lemma 1.1 *When $h_1 < 1$ and $h_2 < \delta$, each positive solution $(x(t), y(t))$ of system (1.2) is bounded. Furthermore, there exists a $T \geq 0$ such that $0 < x(t) < 1 - h_1$ and $0 \leq y < \frac{\delta - h_2}{\beta}(1 - h_1)$ for $t \geq T$.*

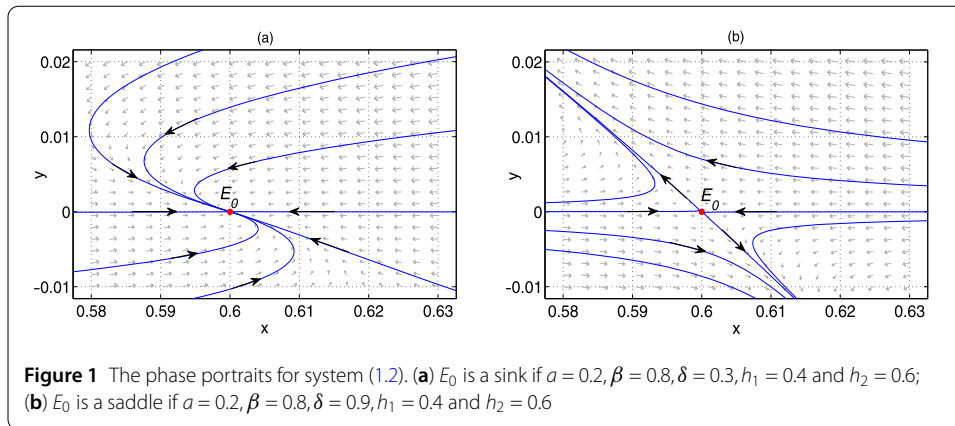
The rest of this paper is organized as follows. In Sect. 2, we analyze the number and property of the equilibria by using the root formula of the cubic equation. In Sect. 3, we discuss the subcritical Hopf bifurcation near the multiple focus and the Bogdanov–Takens bifurcation near a BT singularity. The characteristics of the cusp point and the generalized Hopf points are analyzed simply. Numerical simulations support our results of theoretical analysis. Finally, we end this paper with a conclusion in Sect. 4.

2 Types of equilibria

In this section, for system (1.2) we will study the number and type of equilibria in the region D . It is clear that if $h_1 < 1$ system (1.2) has a boundary equilibrium $E_0 = (1 - h_1, 0)$, which is a sink for $\delta < h_2$ and a saddle for $\delta > h_2$. The corresponding phase portraits are displayed in Fig. 1.

Obviously, a positive equilibrium $E^*(x^*, y^*)$ of system (1.2) should satisfy the following equations:

$$\begin{aligned} 1 - h_1 - x^* - \frac{y^*}{a + x^{*2}} &= 0, \\ y^* - \frac{\delta - h_2}{\beta}x^* &= 0. \end{aligned} \tag{2.1}$$



From Eqs. (2.1), we find that, if positive equilibria exist, then $h_2 < \delta$ and x^* is a root of the equation

$$F(x) = x^3 + (h_1 - 1)x^2 + \left(a + \frac{\delta - h_2}{\beta}\right)x + a(h_1 - 1) = 0. \tag{2.2}$$

To determine the type of $E^*(x^*, y^*)$, the Jacobian matrix J evaluated at $E^*(x^*, y^*)$ is given by

$$J(E^*) = \begin{pmatrix} 1 - h_1 - 2x^* + \frac{(\delta - h_2)(x^{*3} - ax^*)}{\beta(a + x^{*2})^2} & \frac{-x^*}{a + x^{*2}} \\ \frac{(\delta - h_2)^2}{\beta} & -(\delta - h_2) \end{pmatrix}.$$

Thus

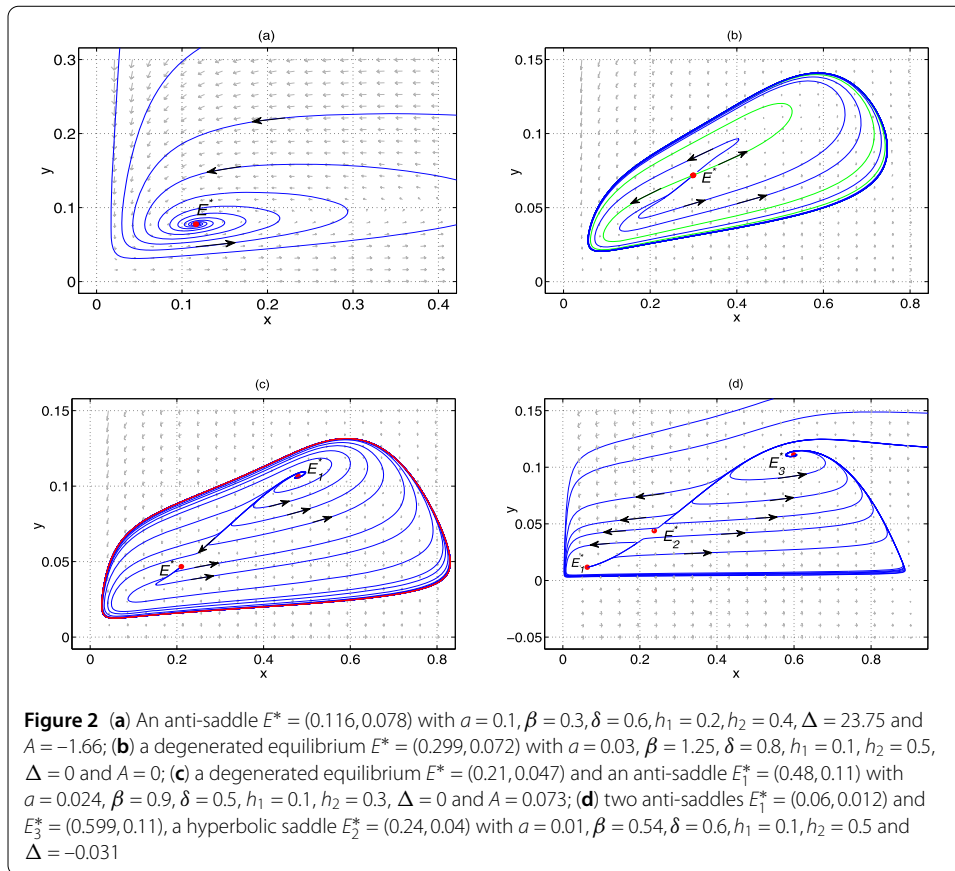
$$\begin{aligned} \text{Det}(J(E^*)) &= (h_2 - \delta)(1 - h_1 - 2x^*) + \frac{2a(\delta - h_2)^2 x^*}{\beta(a + x^{*2})^2} = (\delta - h_2) \frac{x^*}{a + x^{*2}} F'(x^*), \\ \text{Tr}(J(E^*)) &= 1 - h_1 + h_2 - \delta - 2x^* + \frac{(\delta - h_2)(x^{*3} - ax^*)}{\beta(a + x^{*2})^2} \\ &= \frac{x^*}{a + x^{*2}} \left(\frac{\delta - h_2}{\beta} - F'(x^*) \right) - (\delta - h_2). \end{aligned}$$

According to the sign of $\text{Det}(J(E^*))$, the equilibrium $E^*(x^*, y^*)$ can be divided into three types: an anti-saddle equilibrium, a hyperbolic saddle or a degenerated equilibrium if $\text{Det}(J(E^*)) > 0, \text{Det}(J(E^*)) < 0$ or $\text{Det}(J(E^*)) = 0$, respectively. Obviously, the type of $E^*(x^*, y^*)$ is determined by the sign of $F'(x^*)$.

Using the root formula of the third-order equation and estimating the sign of $F'(x^*)$, we can get the following results.

Lemma 2.1 Suppose $h_1 < 1, h_2 < \delta, A = (h_1 - 1)^2 - 3(a + \frac{\delta - h_2}{\beta})$ and $\Delta = -4A^3 + (h_1 - 1)^2[3A + 27a - (h_1 - 1)^2]^2$.

- (a) If $\Delta > 0$, then system (1.2) has a unique positive equilibrium $E^*(x^*, y^*)$, which is an anti-saddle equilibrium whatever the sign of A is.
- (b) If $\Delta = 0, A = 0$, then system (1.2) has a unique positive equilibrium $E^*(x^*, y^*) = (\frac{1-h_1}{3}, \frac{(\delta-h_2)(1-h_1)}{3\beta})$, which is degenerated.



(c) If $\Delta = 0, A > 0$ and $\max\{\frac{(h_1-1)^2-4A}{27}, 0\} < a < \frac{(h_1-1)^2-A}{27}$, then the system (1.2) has two positive equilibria: an anti-saddle equilibrium

$$E_1^*(x_1^*, y_1^*) = \left(\frac{(1-h_1)[4A+27a-(h_1-1)^2]}{3A}, \frac{(\delta-h_2)(1-h_1)[4A+27a-(h_1-1)^2]}{3\beta A} \right)$$

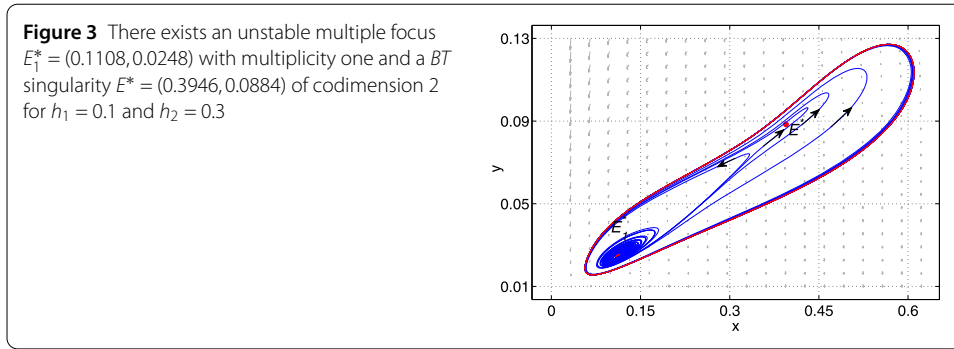
and a degenerated equilibrium

$$E^*(x^*, y^*) = \left(\frac{(1-h_1)[(h_1-1)^2-A-27a]}{6A}, \frac{(\delta-h_2)(1-h_1)[(h_1-1)^2-A-27a]}{6\beta A} \right).$$

(d) If $\Delta < 0$, then system (1.2) has three positive equilibria $E_1^*(x_1^*, y_1^*), E_2^*(x_2^*, y_2^*)$ and $E_3^*(x_3^*, y_3^*)$. E_1^* and E_3^* are anti-saddle equilibria and E_2^* is a hyperbolic saddle.

The detailed proof of Lemma 2.1 is given in the appendix. The phase portraits for the four cases are exhibited in Fig. 2.

Next, we discuss the case (c) of Lemma 2.1 and look for some parameter values such that system (1.2) has a degenerated equilibrium $E^*(x^*, y^*)$ with $\text{Det}(J(E^*)) = 0$ and $\text{Tr}(J(E^*)) = 0$ and a non-hyperbolic equilibrium $E_1^*(x_1^*, y_1^*)$ with $\text{Det}(J(E_1^*)) > 0$ and $\text{Tr}(J(E_1^*)) = 0$.



From $\text{Det}(J(E^*)) = 0$ and $\text{Tr}(J(E^*)) = 0$, we can get

$$\begin{aligned} x^* &= 1 - h_1 - \delta + h_2, & y^* &= \frac{\delta - h_2}{\beta} x^*, \\ a &= \frac{(1 - h_1 - \delta + h_2)^2 [2(\delta - h_2) + h_1 - 1]}{1 - h_1}, & \beta &= \frac{1 - h_1}{2(\delta - h_2)(1 - h_1 - \delta + h_2)}, \end{aligned} \tag{2.3}$$

where $(\delta - h_2) < 1 - h_1 < 2(\delta - h_2)$.

Thus when a, β satisfy (2.3) and $3(\delta - h_2) \neq 2(1 - h_1)$, system (1.2) has two positive equilibria

$$\begin{aligned} E_1^* &= \left(2(\delta - h_2) + h_1 - 1, \frac{2(\delta - h_2)^2 (2\delta - 2h_2 + h_1 - 1)(1 - h_1 - \delta + h_2)}{1 - h_1} \right) \text{ and} \\ E^* &= \left(1 - h_1 - \delta + h_2, \frac{2(\delta - h_2)^2 (1 - h_1 - \delta + h_2)^2}{1 - h_1} \right). \end{aligned}$$

Furthermore, when E_1^* satisfies $\text{Det}(J(E_1^*)) > 0$ and $\text{Tr}(J(E_1^*)) = 0$, the following conclusions hold.

Theorem 2.2 *If $0 < h_1 < 1$ and $(a, \beta, \delta) = (\frac{41\sqrt{17}-169}{2}(1 - h_1)^2, \frac{4+\sqrt{17}}{4(1-h_1)}, \frac{\sqrt{17}-3}{2}(1 - h_1) + h_2)$, then (1.2) has two positive equilibria*

$$\begin{aligned} E_1^* &= ((\sqrt{17} - 4)(1 - h_1), (114\sqrt{17} - 470)(1 - h_1)^3) \text{ and} \\ E^* &= \left(\frac{5 - \sqrt{17}}{2}(1 - h_1), (264 - 64\sqrt{17})(1 - h_1)^3 \right). \end{aligned}$$

Moreover, (i) E_1^* is an unstable multiple focus with multiplicity one. (ii) E^* is a codimension 2 BT singularity. The phase diagram is shown in Fig. 3.

Proof When a, β and δ satisfy the conditions in Theorem 2.2, system (1.2) becomes

$$\begin{aligned} \dot{x} &= x(1 - x) - \frac{2xy}{(41\sqrt{17} - 169)(1 - h_1)^2 + 2x^2} - h_1 x, \\ \dot{y} &= y \left(\frac{\sqrt{17} - 3}{2}(1 - h_1) - \frac{4 + \sqrt{17}}{4(1 - h_1)} \frac{y}{x} \right). \end{aligned} \tag{2.4}$$

Obviously, (2.4) has two equilibria E_1^* and E^* as stated above.

(1) To prove (i), let $u = x - (\sqrt{17} - 4)(1 - h_1)$, $v = y - (114\sqrt{17} - 470)(1 - h_1)^3$ and Taylor expand (2.4), thus we get

$$\begin{aligned} \dot{u} &= \frac{\sqrt{17} - 3}{2}(1 - h_1)u - \frac{13 + 3\sqrt{17}}{8(1 - h_1)}v + 3u^2 - \frac{45 + 11\sqrt{17}}{16(1 - h_1)^2}uv \\ &\quad - \frac{85 + 19\sqrt{17}}{8(1 - h_1)}u^3 + \frac{235 + 57\sqrt{17}}{4(1 - h_1)^3}u^2v + O(|u, v|^4), \\ \dot{v} &= (50\sqrt{17} - 206)(1 - h_1)^3u + \frac{3 - \sqrt{17}}{2}(1 - h_1)v \\ &\quad + (6\sqrt{17} - 26)(1 - h_1)^2u^2 + (\sqrt{17} + 5)uv \\ &\quad - \frac{33 + 8\sqrt{17}}{4(1 - h_1)^2}v^2 + (2\sqrt{17} + 2)(1 - h_1)u^3 \\ &\quad - \frac{37 + 9\sqrt{17}}{1 - h_1}u^2v + \frac{268 + 65\sqrt{17}}{4(1 - h_1)^3}uv^2 + O(|u, v|^4). \end{aligned} \tag{2.5}$$

Suppose

$$x = \frac{\sqrt{3526\sqrt{17} - 14,538}}{2}(1 - h_1)^2u, \quad y = \frac{45 - 11\sqrt{17}}{2}(1 - h_1)^2u + v,$$

then (2.5) can be changed into

$$\dot{x} = -\omega_0 y + f(x, y), \quad \dot{y} = \omega_0 x + g(x, y), \tag{2.6}$$

where $\omega_0 = \frac{\sqrt{22\sqrt{17} - 90}}{2}(1 - h_1)$ and

$$\begin{aligned} f(x, y) &= \frac{\sqrt{7269 + 1763\sqrt{17}}}{8(1 - h_1)^2}x^2 - \frac{45 + 11\sqrt{17}}{16(1 - h_1)^2}xy + \frac{11,351 + 2753\sqrt{17}}{1024(1 - h_1)^5}x^3 \\ &\quad + \frac{\sqrt{401,460,573 + 97,368,491\sqrt{17}}}{32(1 - h_1)^5}x^2y + O(|x, y|^4), \\ g(x, y) &= -\frac{235 + 57\sqrt{17}}{16(1 - h_1)^2}x^2 + \frac{\sqrt{133,205 + 32,307\sqrt{17}}}{16(1 - h_1)^2}xy - \frac{33 + 8\sqrt{17}}{4(1 - h_1)^2}y^2 \\ &\quad + \frac{\sqrt{151,456,733,853 + 36,733,653,611\sqrt{17}}}{1024(1 - h_1)^5}x^3 \\ &\quad - \frac{86,243 + 20,917\sqrt{17}}{64(1 - h_1)^5}x^2y + \frac{\sqrt{2,088,374,221 + 50,650,514\sqrt{17}}}{64(1 - h_1)^5}xy^2 \\ &\quad + O(|x, y|^4). \end{aligned}$$

The first Lyapunov number [23] can be expressed as

$$\begin{aligned} \text{Re } c_1 &= \frac{1}{16} \left\{ (f_{xxx} + f_{xyy} + g_{xxy} + g_{yyy}) \right. \\ &\quad \left. + \frac{1}{\omega_0} [f_{xy}(f_{xx} + f_{yy}) - g_{xy}(g_{xx} + g_{yy}) - f_{xx}g_{xx} + f_{yy}g_{yy}] \right\} \Big|_{x=y=0} \end{aligned}$$

$$= \frac{1,428,479 + 346,457\sqrt{17}}{8192(1 - h_1)^5} > 0,$$

thus E_1^* is an unstable multiple focus with multiplicity one.

(2) To prove (ii), let $x_1 = x - \frac{5-\sqrt{17}}{2}(1 - h_1)$, $x_2 = y - (264 - 64\sqrt{17})(1 - h_1)^3$ and expand (2.4) in a power series at the origin, thus (2.4) becomes

$$\begin{aligned} \dot{x}_1 &= \frac{\sqrt{17} - 3}{2}(1 - h_1)x_1 - \frac{\sqrt{17} + 4}{4(1 - h_1)}x_2 - \frac{\sqrt{17} + 9}{8}x_1^2 \\ &\quad + \frac{7\sqrt{17} + 29}{16(1 - h_1)^2}x_1x_2 + O(|x_1, x_2|^3), \\ \dot{x}_2 &= (50\sqrt{17} - 206)(1 - h_1)^3x_1 - \frac{(\sqrt{17} - 3)(1 - h_1)}{2}x_2 \\ &\quad + (45 - 11\sqrt{17})(1 - h_1)^2x_1^2 + \frac{\sqrt{17} + 1}{2}x_1x_2 \\ &\quad - \frac{9\sqrt{17} + 37}{16(1 - h_1)^2}x_2^2 + O(|x_1, x_2|^3). \end{aligned} \tag{2.7}$$

Making the affine transformation

$$y_1 = \frac{25\sqrt{17} + 103}{32(1 - h_1)^3}x_2, \quad y_2 = x_1 - \frac{7\sqrt{17} + 29}{16(1 - h_1)^2}x_2,$$

we obtain

$$\begin{aligned} \dot{y}_1 &= y_2 - \frac{\sqrt{17} + 5}{4(1 - h_1)}y_2^2 + O(|y_1, y_2|^3), \\ \dot{y}_2 &= \frac{19 - 5\sqrt{17}}{8}(1 - h_1)^2y_1^2 - \frac{\sqrt{17} + 1}{4}(1 - h_1)y_1y_2 + \frac{\sqrt{17} - 7}{8}y_2^2 + O(|y_1, y_2|^3). \end{aligned} \tag{2.8}$$

By a C^∞ change of variables

$$z_1 = y_1 - \frac{\sqrt{17} - 7}{16}y_1^2 + \frac{\sqrt{17} + 5}{4(1 - h_1)}y_1y_2, \quad z_2 = y_2 - \frac{\sqrt{17} - 7}{8}y_1y_2,$$

system (2.8) becomes

$$\begin{aligned} \dot{z}_1 &= z_2 + O(|z_1, z_2|^3), \\ \dot{z}_2 &= \frac{19 - 5\sqrt{17}}{8}(1 - h_1)^2z_1^2 - \frac{\sqrt{17} + 1}{4}(1 - h_1)z_1z_2 + O(|z_1, z_2|^3). \end{aligned} \tag{2.9}$$

Suppose $\rho_1 = \frac{19-5\sqrt{17}}{8}(1 - h_1)^2$ and $\rho_2 = -\frac{\sqrt{17}+1}{4}(1 - h_1)$, then $\rho_1\rho_2 = \frac{33-7\sqrt{17}}{16}(1 - h_1)^3 \neq 0$ for $0 < h_1 < 1$. Hence E^* is a *BT* singularity of codimension 2. \square

3 Bifurcations

In this section, we study the subcritical Hopf bifurcation in a neighborhood of E_1^* and the Bogdanov–Takens bifurcation in a neighborhood of E^* . Now we carry out bifurcation analysis for system (1.2) by choosing h_1 and h_2 as bifurcation parameters. When the

conditions of Theorem 2.2 are satisfied, the unfolding system of (1.2) is given by

$$\begin{aligned} \dot{x} &= x(1-x) - \frac{2xy}{(41\sqrt{17}-169)(1-h_1)^2+2x^2} - (h_1+\mu_1)x, \\ \dot{y} &= y\left(\frac{\sqrt{17}-3}{2}(1-h_1)+h_2 - \frac{4+\sqrt{17}}{4(1-h_1)}\frac{y}{x}\right) - (h_2+\mu_2)y, \end{aligned} \tag{3.1}$$

where μ_1 and μ_2 are small parameters.

Through analysis, we have the following conclusions.

Theorem 3.1 *When μ_1 and μ_2 vary near the origin, system (3.1) undergoes a subcritical Hopf bifurcation in a small neighborhood of E_1^* and a Bogdanov–Takens bifurcation in a small neighborhood of E^* . Hence, when h_1 and h_2 vary, system (1.2) may have an unstable closed cycle around E_1^* , and an unstable closed cycle or an unstable homoclinic loop around E^* .*

Proof If $\mu_1 = \mu_2 = 0$, then (3.1) has two equilibria E_1^* and E^* , whose types are discussed in Theorem 2.2.

(1) First we verify that system (3.1) experiences a subcritical Hopf bifurcation around E_1^* when (μ_1, μ_2) varies in a small neighborhood of the origin. If $(\mu_1, \mu_2) \neq (0, 0)$, (3.1) has an equilibrium with the following form:

$$\begin{aligned} E_1 &= (x_1, y_1) \\ &= \left((\sqrt{17}-4)(1-h_1) + \omega, \frac{7\sqrt{17}-29}{2}[(3+\sqrt{17})\mu_2 - 4(1-h_1)](1-h_1)x_1 \right). \end{aligned} \tag{3.2}$$

Here ω is an infinitely small quantity for μ_1 and μ_2 small enough.

Substituting (3.2) into (3.1), one can find that x_1 should satisfy the following equations:

$$\begin{aligned} x^3 + (h_1 + \mu_1 - 1)x^2 + \left[\frac{1}{16}(13\sqrt{17}-53)(8h_1 + 9\mu_2 + \mu_2\sqrt{17}-8)(h_1-1) \right]x \\ + \frac{1}{2}(41\sqrt{17}-169)(h_1 + \mu_1 - 1)(h_1 - 1)^2 = 0, \end{aligned} \tag{3.3}$$

$$\begin{aligned} \text{Tr}(J(E_1)) &= \frac{5-\sqrt{17}}{2}(1-h_1) - 2x_1 \\ &+ \frac{(44+12\sqrt{17})(1-h_1)^2[(169+41\sqrt{17})x_1^3 - 8(1-h_1)^2x_1]}{[(169+41\sqrt{17})x_1^2 + 8(1-h_1)^2]^2} - \mu_1 \\ &+ \left(1 - \frac{(84+20\sqrt{17})(1-h_1)[(169+41\sqrt{17})x_1^3 - 8(1-h_1)^2x_1]}{[(169+41\sqrt{17})x_1^2 + 8(1-h_1)^2]^2} \right) \mu_2, \end{aligned}$$

$$\begin{aligned} \text{Det}(J(E_1)) &= \left(1 - h_1 - \mu_1 - 2x_1 \right. \\ &\left. - \frac{(11+3\sqrt{17})(1-h_1)[(3+\sqrt{17})\mu_2 - 4(1-h_1)][(169+41\sqrt{17})x_1^3 - 8(1-h_1)^2x_1]}{[(169+41\sqrt{17})x_1^2 + 8(1-h_1)^2]^2} \right) \end{aligned}$$

$$\begin{aligned} & \times \left(\mu_2 + \frac{3 - \sqrt{17}}{2}(1 - h_1) \right) \\ & + \frac{(9 + \sqrt{17})(1 - h_1)[(3 + \sqrt{17})\mu_2 - 4(1 - h_1)]^2 x_1}{4[(169 + 41\sqrt{17})x_1^2 + 8(1 - h_1)^2]}. \end{aligned}$$

Letting $\text{Tr}(J(E_1)) = 0, \text{Det}(J(E_1)) > 0$ and according to (3.3), we can get

$$\begin{aligned} \mu_1 = & (-2\omega^5 + 2(7\sqrt{17} - 27)(1 - h_1)\omega^4 - 2(349\sqrt{17} - 1439)(1 - h_1)^2\omega^3 \\ & + 8(1137\sqrt{17} - 4688)(1 - h_1)^3\omega^2 - (37,001\sqrt{17} - 152,559)(1 - h_1)^4\omega) \\ & / (2\omega^4 - 8(\sqrt{17} - 4)(1 - h_1)\omega^3 + 2(185\sqrt{17} - 763)(1 - h_1)^2\omega^2 \\ & - 4(983\sqrt{17} - 4053)(1 - h_1)^3\omega + (5873\sqrt{17} - 24,215)(1 - h_1)^4), \\ \mu_2 = & (2\omega^5 + (11\sqrt{17} - 43)(1 - h_1)\omega^4 - 2(25\sqrt{17} - 103)(1 - h_1)^2\omega^3 \\ & + 8(252\sqrt{17} - 1039)(1 - h_1)^3\omega^2 + 7(2575\sqrt{17} - 10,617)(1 - h_1)^4\omega) \\ & / (2\omega^4 - 8(\sqrt{17} - 4)(1 - h_1)\omega^3 + 2(185\sqrt{17} - 763)(1 - h_1)^2\omega^2 \\ & + 4(983\sqrt{17} - 4053)(1 - h_1)^3\omega + (5873\sqrt{17} - 24,215)(1 - h_1)^4). \end{aligned} \tag{3.4}$$

Substituting (3.2) and (3.4) into $\text{Det}(J(E_1))$, we obtain $\text{Det}(J(E_1)) > 0$ if and only if

$$\frac{463\sqrt{17} + 1783}{2}\omega^2 + 2(3\sqrt{17} - 22)(1 - h_1)\omega + \frac{11\sqrt{17} - 45}{2}(1 - h_1)^2 > 0. \tag{3.5}$$

The discriminant of inequality (3.5) is always negative for $h_1 < 1$, so $\text{Det}(J(E_1)) > 0$ for all small ω . The Hopf bifurcation curve of system (3.1) at E_1^* is defined by

$$H_1 = \{(\mu_1, \mu_2) | \mu_1 \text{ and } \mu_2 \text{ are given by (3.4) and } \omega \text{ is sufficiently small}\}.$$

Due to $\lim_{\omega \rightarrow 0} \frac{\mu_2}{\mu_1} = \frac{35 + 7\sqrt{17}}{41 + 13\sqrt{17}}$, thus the approximate expression of H_1 is given by $\mu_2 = \frac{35 + 7\sqrt{17}}{41 + 13\sqrt{17}}\mu_1$ in a small neighborhood of the origin.

(2) Now we prove that system (3.1) undergoes a Bogdanov–Takens bifurcation at the BT singularity E^* . First translate E^* to the origin by letting $x_1 = x - \frac{5 - \sqrt{17}}{2}(1 - h_1)$ and $x_2 = y - (264 - 64\sqrt{17})(1 - h_1)^3$ and Taylor expand system (3.1), then we have

$$\begin{aligned} \dot{x}_1 = & \frac{\sqrt{17} - 5}{2}(1 - h_1)\mu_1 - \frac{\sqrt{17} - 3}{8}(\sqrt{17}\mu_1 + 4h_1 + 3\mu_1 - 4)x_1 - \frac{4 + \sqrt{17}}{4(1 - h_1)}x_2 \\ & - \frac{9 + \sqrt{17}}{8}x_1^2 + \frac{29 + 7\sqrt{17}}{16(1 - h_1)^2}x_1x_2 + O(|x_1, x_2|^3), \\ \dot{x}_2 = & 8\mu_2(8\sqrt{17} - 33)(1 - h_1)^3 + (50\sqrt{17} - 206)(1 - h_1)^3x_1 \\ & - \frac{\sqrt{17} - 3}{8}(\sqrt{17}\mu_2 - 4h_1 + 3\mu_2 + 4)x_2 \\ & + (45 - 11\sqrt{17})(1 - h_1)^2x_1^2 + \frac{1 + \sqrt{17}}{2}x_1x_2 - \frac{37 + 9\sqrt{17}}{16(1 - h_1)^2}x_2^2 + O(|x_1, x_2|^3). \end{aligned} \tag{3.6}$$

With an affine transformation $y_1 = x_1, y_2 = \frac{\sqrt{17}-3}{2}(1-h_1)x_1 - \frac{4+\sqrt{17}}{4(1-h_1)}x_2$, system (3.6) becomes

$$\begin{aligned} \dot{y}_1 &= \frac{\sqrt{17}-5}{2}(1-h_1)\mu_1 - \mu_1 y_1 + y_2 - \frac{1+\sqrt{17}}{8}y_1^2 - \frac{3+\sqrt{17}}{4(1-h_1)}y_1 y_2 + O(|y_1, y_2|^3), \\ \dot{y}_2 &= (8-2\sqrt{17})(\mu_1 - \mu_2)(1-h_1)^2 - \frac{(\sqrt{17}-3)(\mu_1 - \mu_2)}{2}(1-h_1)y_1 \\ &\quad - \mu_2 y_2 + \frac{\sqrt{17}-7}{8}(1-h_1)y_1^2 \\ &\quad - y_1 y_2 + \frac{5+\sqrt{17}}{4(1-h_1)}y_2^2 + O(|y_1, y_2|^3). \end{aligned} \tag{3.7}$$

Under a C^∞ transformation of coordinates

$$z_1 = y_1, \quad z_2 = \frac{\sqrt{17}-5}{2}(1-h_1)\mu_1 - \mu_1 y_1 + y_2 - \frac{1+\sqrt{17}}{8}y_1^2 - \frac{3+\sqrt{17}}{4(1-h_1)}y_1 y_2,$$

system (3.7) can be transformed into

$$\begin{aligned} \dot{z}_1 &= z_2 + O(|z_1, z_2|^3), \\ \dot{z}_2 &= \beta_0 + \beta_1 z_1 + \frac{\sqrt{17}-5}{8}[(5+\sqrt{17})\mu_2 - 2\mu_1]z_2 + \beta_2 z_1^2 \\ &\quad + \frac{(5+\sqrt{17})[(5+3\sqrt{17})\mu_1 - 8(1-h_1)]}{32(1-h_1)}z_1 z_2 + \frac{1}{2(1-h_1)}z_2^2 + O(|z_1, z_2|^3), \end{aligned} \tag{3.8}$$

where

$$\begin{aligned} \beta_0 &= \frac{\sqrt{17}-4}{2}(1-h_1)(\mu_1 - \mu_2)[(3+\sqrt{17})\mu_1 - 4(1-h_1)], \\ \beta_1 &= \frac{\sqrt{17}-3}{16}[(19+5\sqrt{17})\mu_1^2 - (6+2\sqrt{17})\mu_1 \mu_2 - 8(1-h_1)\mu_1 \\ &\quad + (10-2\sqrt{17})(1-h_1)\mu_2], \\ \beta_2 &= \frac{1}{128(1-h_1)}(\sqrt{17}-7)[-(161+39\sqrt{17})\mu_1^2 - (24+8\sqrt{17})(1-h_1)\mu_1 \\ &\quad + (40+8\sqrt{17})(1-h_1)\mu_2 + 16(1-h_1)^2]. \end{aligned}$$

By another C^∞ change $X_1 = z_1 - \frac{1}{4(1-h_1)}z_2^2, X_2 = z_2 - \frac{1}{2(1-h_1)}z_1 z_2$, system (3.8) becomes

$$\begin{aligned} \dot{X}_1 &= X_2 + O(|X_1, X_2|^3), \\ \dot{X}_2 &= \beta_0 - \frac{2\beta_1 h_1 + \beta_0 - 2\beta_1}{2(1-h_1)}X_1 + \frac{\sqrt{17}-5}{8}[(5+\sqrt{17})\mu_2 - 2\mu_1]X_2 \\ &\quad + \psi X_1^2 + \frac{(5+\sqrt{17})[(5+3\sqrt{17})\mu_1 - 8(1-h_1)]}{32(1-h_1)}X_1 X_2 \\ &\quad + O(|X_1, X_2|^3), \end{aligned} \tag{3.9}$$

where $\psi = \frac{8\beta_2 h_1^2 + 2(\beta_1 - 8\beta_2)h_1 - \beta_0 - 2\beta_1 + 8\beta_2}{8(1-h_1)^2}$.

Consider the C^∞ change $Y_1 = X_1, Y_2 = X_2 + O(|X_1, X_2|^3)$ and system (3.9) can be changed into

$$\begin{aligned} \dot{Y}_1 &= Y_2, \\ \dot{Y}_2 &= \beta_0 - \frac{2\beta_1 h_1 + \beta_0 - 2\beta_1}{2(1-h_1)} Y_1 + \frac{\sqrt{17}-5}{8} [(5 + \sqrt{17})\mu_2 - 2\mu_1] Y_2 \\ &\quad + \psi Y_1^2 + \frac{(5 + \sqrt{17})[(5 + 3\sqrt{17})\mu_1 - 8(1-h_1)]}{32(1-h_1)} Y_1 Y_2 + O(|Y_1, Y_2|^3). \end{aligned} \tag{3.10}$$

Substituting the expressions of β_0, β_1 and β_2 into ψ , we have $\psi < 0$ for any small μ_1 and μ_2 . Under the following change:

$$Z_1 = Y_1, \quad Z_2 = \frac{Y_2}{\sqrt{-\psi}}, \quad \tau = \sqrt{-\psi} t,$$

system (3.10) becomes

$$\begin{aligned} \dot{Z}_1 &= Z_2, \\ \dot{Z}_2 &= \frac{\beta_0}{-\psi} + \frac{2\beta_1 h_1 + \beta_0 - 2\beta_1}{2(1-h_1)\psi} Z_1 + \frac{\sqrt{17}-5}{8\sqrt{-\psi}} [(5 + \sqrt{17})\mu_2 - 2\mu_1] Z_2 \\ &\quad - Z_1^2 + \frac{(5 + \sqrt{17})[(5 + 3\sqrt{17})\mu_1 - 8(1-h_1)]}{32(1-h_1)\sqrt{-\psi}} Z_1 Z_2 \\ &\quad + O(|Z_1, Z_2|^3). \end{aligned} \tag{3.11}$$

The transformation $U = Z_1 - \frac{2\beta_1 h_1 + \beta_0 - 2\beta_1}{4(1-h_1)\psi}, V = Z_2$ brings (3.11) into the form

$$\begin{aligned} \dot{U} &= V, \\ \dot{V} &= \frac{(2\beta_1 h_1 + \beta_0 - 2\beta_1)^2}{16(1-h_1)^2 \psi^2} - \frac{\beta_0}{\psi} + \phi V - U^2 \\ &\quad + \frac{(5 + \sqrt{17})[(5 + 3\sqrt{17})\mu_1 - 8(1-h_1)]}{32(1-h_1)\sqrt{-\psi}} UV + O(|U, V|^3), \end{aligned} \tag{3.12}$$

where $\phi = \frac{(5 + \sqrt{17})(2\beta_1 h_1 + \beta_0 - 2\beta_1)[(5 + 3\sqrt{17})\mu_1 - 8(1-h_1)]}{128(1-h_1)^2 \psi \sqrt{-\psi}} + \frac{(\sqrt{17}-5)[(5 + \sqrt{17})\mu_2 - 2\mu_1]}{8\sqrt{-\psi}}$.

The derivatives of (3.11) and (3.12) are about time τ . For μ_1 small enough we make the following transformation:

$$\begin{aligned} x &= - \left(\frac{(5 + \sqrt{17})[(5 + 3\sqrt{17})\mu_1 - 8(1-h_1)]}{32(1-h_1)\sqrt{-\psi}} \right)^2 U, \\ y &= \left(\frac{(5 + \sqrt{17})[(5 + 3\sqrt{17})\mu_1 - 8(1-h_1)]}{32(1-h_1)\sqrt{-\psi}} \right)^3 V, \\ t &= - \frac{32(1-h_1)\sqrt{-\psi}}{(5 + \sqrt{17})[(5 + 3\sqrt{17})\mu_1 - 8(1-h_1)]} \tau, \end{aligned}$$

then system (3.12) becomes

$$\begin{aligned} \dot{x} &= y, \\ \dot{y} &= \eta_1(\mu_1, \mu_2) + \eta_2(\mu_1, \mu_2)y + x^2 + xy + O(|x, y|^3), \end{aligned} \tag{3.13}$$

where the derivatives are about time t and the expressions of $\eta_1(\mu_1, \mu_2)$ and $\eta_2(\mu_1, \mu_2)$ are given by

$$\begin{aligned} \eta_1(\mu_1, \mu_2) &= \frac{(53 + 13\sqrt{17})^2((5 + 3\sqrt{17})\mu_1 - 8(1 - h_1))^4}{134,217,728(1 - h_1)^4 Q(\mu_1, \mu_2)^4} \\ &\quad \times \left[8(13\sqrt{17} - 53)(1 - h_1)(\mu_1 - \mu_2)(3\mu_1 + \sqrt{17}\mu_1 + 4h_1 - 4)Q(\mu_1, \mu_2) \right. \\ &\quad \left. + \frac{33\sqrt{17} - 137}{4}(3\sqrt{17}\mu_1 + 11\mu_1 - \sqrt{17}\mu_2 - 3\mu_2 + 4h_1 - 4)^2\mu_1^2 \right], \\ \eta_2(\mu_1, \mu_2) &= \frac{(5\mu_1 + 3\sqrt{17}\mu_1 + 8h_1 - 8)(5 + \sqrt{17})}{1024(1 - h_1)^2 Q(\mu_1, \mu_2)^2} \\ &\quad \times \left[4(\sqrt{17} - 5)(1 - h_1)(-2\mu_1\sqrt{17}\mu_2 + 5\mu_2)Q(\mu_1, \mu_2) \right. \\ &\quad \left. - \frac{1}{2}(3\sqrt{17}\mu_1 + 11\mu_1 - \sqrt{17}\mu_2 - 3\mu_2 + 4h_1 - 4)(3\sqrt{17}\mu_1 + 5\mu_1 + 8h_1 - 8)\mu_1 \right], \\ Q(\mu_1, \mu_2) &= \frac{1}{16(1 - h_1)} \left[(46 + 14\sqrt{17})\mu_1^2 - (\sqrt{17} - 9)\mu_1\mu_2 + 2(5\sqrt{17} - 9)(1 - h_1)\mu_1 \right. \\ &\quad \left. - 2(5\sqrt{17} - 7)(1 - h_1)\mu_2 \right. \\ &\quad \left. + 2(\sqrt{17} - 7)(1 - h_1)^2 \right]. \end{aligned}$$

We can check

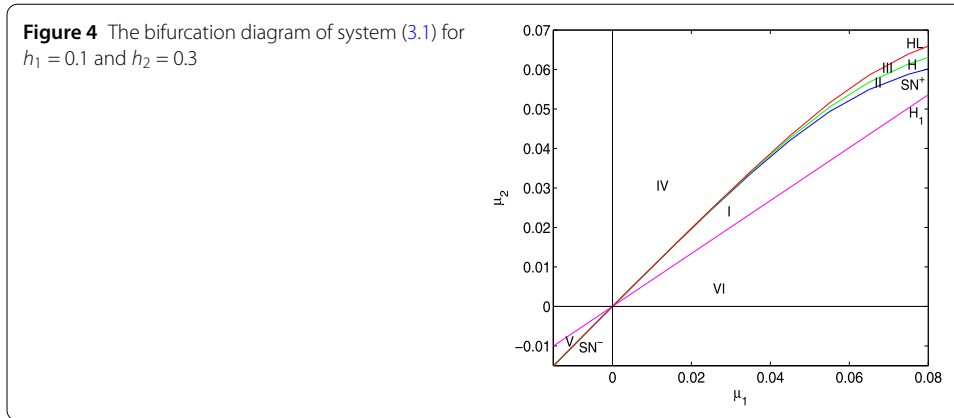
$$\left| \frac{\partial(\eta_1, \eta_2)}{\partial(\mu_1, \mu_2)} \right|_{\mu_1=\mu_2=0} = \frac{4299\sqrt{17} + 17,725}{64(1 - h_1)^2} \neq 0,$$

for $0 < h_1 < 1$, which indicates that above parameter transformation is regular at $(0, 0)$.

From the results in [2] and [27], we know that system (3.1) undergoes a Bogdanov–Takens bifurcation when (μ_1, μ_2) varies in a small neighborhood of the origin, and the local expressions of the bifurcation curves in a small neighborhood of the origin are given by:

- (a) the saddle-node bifurcation curve

$$\begin{aligned} SN = \left\{ (\mu_1, \mu_2) \mid \eta_1 = 0, \text{ i.e., } \mu_1 - \mu_2 + \frac{(19\sqrt{17} - 43)\mu_1^2}{32(1 - h_1)} \right. \\ \left. - \frac{(53\sqrt{17} + 35)\mu_1\mu_2}{16(1 - h_1)} + \frac{3(7\sqrt{17} + 9)\mu_2^2}{8(1 - h_1)} + O(|\mu_1, \mu_2|^3) = 0 \right\}, \end{aligned}$$



which includes $SN^+ = \{(\mu_1, \mu_2) | \eta_1 = 0, \eta_2 > 0\}$ and $SN^- = \{(\mu_1, \mu_2) | \eta_1 = 0, \eta_2 < 0\}$;
 (b) the Hopf bifurcation curve

$$\begin{aligned}
 H &= \{(\mu_1, \mu_2) | \eta_2 = \sqrt{-\eta_1}, \eta_1 < 0\} \\
 &= \left\{ (\mu_1, \mu_2) \mid \mu_1 - \mu_2 + \frac{5(7\sqrt{17} - 23)\mu_1^2}{16(1 - h_1)} - \frac{(73\sqrt{17} - 33)\mu_1\mu_2}{16(1 - h_1)} \right. \\
 &\quad \left. + \frac{(23\sqrt{17} + 21)\mu_2^2}{8(1 - h_1)} + O(|\mu_1, \mu_2|^3) = 0, \eta_1 < 0 \right\};
 \end{aligned}$$

(c) the homoclinic bifurcation curve

$$\begin{aligned}
 HL &= \left\{ (\mu_1, \mu_2) \mid \eta_2 = \frac{5}{7}\sqrt{-\eta_1}, \eta_1 < 0 \right\} \\
 &= \left\{ (\mu_1, \mu_2) \mid \mu_1 - \mu_2 + \frac{(1487\sqrt{17} - 5119)\mu_1^2}{400(1 - h_1)} - \frac{(2305\sqrt{17} - 2457)\mu_1\mu_2}{400(1 - h_1)} \right. \\
 &\quad \left. + \frac{(623\sqrt{17} + 381)\mu_2^2}{200(1 - h_1)} + O(|\mu_1, \mu_2|^3) = 0, \eta_1 < 0 \right\};
 \end{aligned}$$

(d) the Hopf bifurcation curve of system (3.1) at E_1^* is

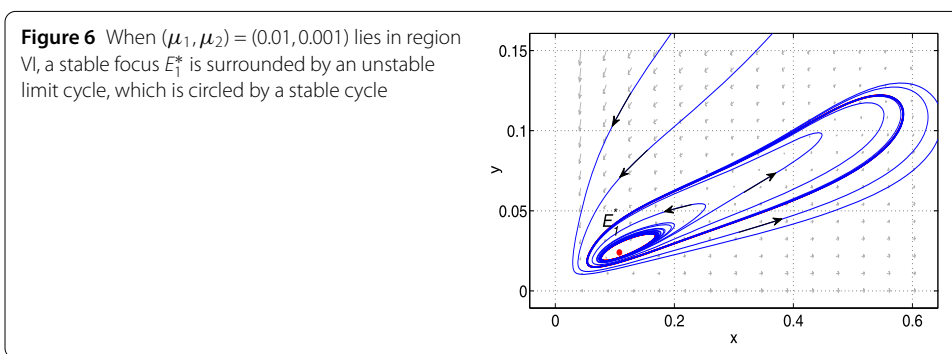
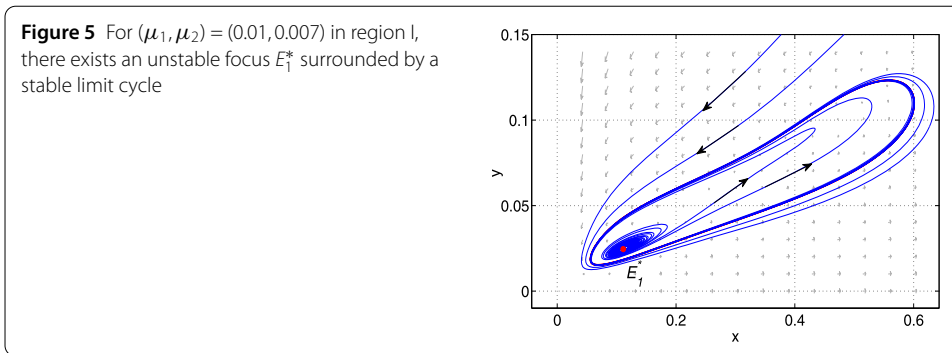
$$H_1 = \left\{ (\mu_1, \mu_2) \mid \mu_2 = \frac{35 + 7\sqrt{17}}{41 + 13\sqrt{17}}\mu_1 \right\}.$$

The sketches of these bifurcation curves are displayed in Fig. 4.

Due to $\eta_2 < 0$ around the origin, H and HL are nonexistent in the third quadrant of Fig. 4, so only SN^- and H_1 are considered in this part. Obviously, the neighborhood of the origin in the (μ_1, μ_2) -plane is divided into six parts by H_1, SN^+, H, HL and SN^- .

When (μ_1, μ_2) lies in region I, system (3.1) has an unstable focus E_1^* . By Lemma 1.1 and the Poincaré–Bendixson theorem, it can be proved that there exists a stable limit cycle. The corresponding phase portrait is depicted in Fig. 5. From the biological point of view, we know that the prey and the predators can coexist and will periodically fluctuate along this cycle eventually.

When (μ_1, μ_2) lies on the curve H_1 , the stable limit cycle still exists and the equilibrium E_1^* turns into an unstable multiple focus with multiplicity one. When (μ_1, μ_2) crosses H_1

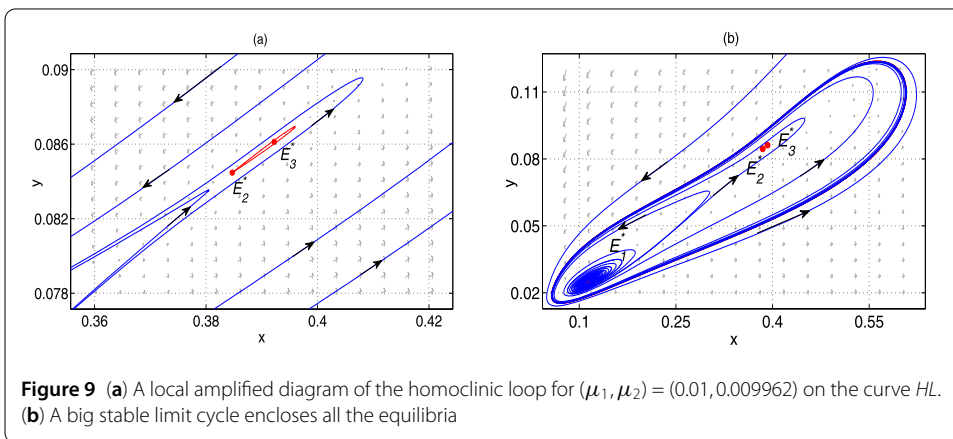
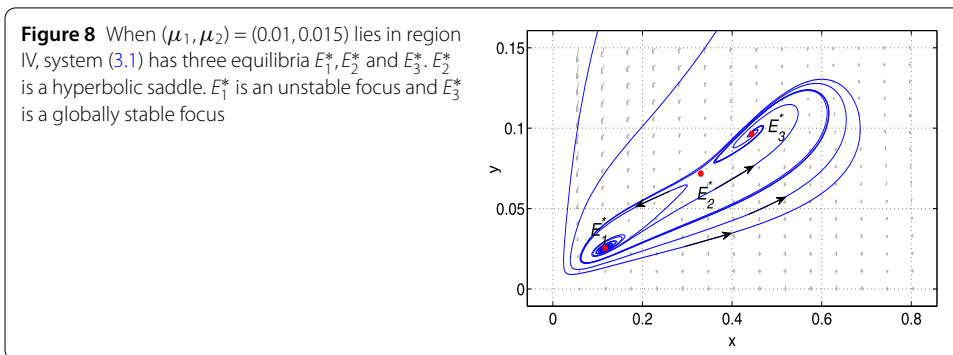
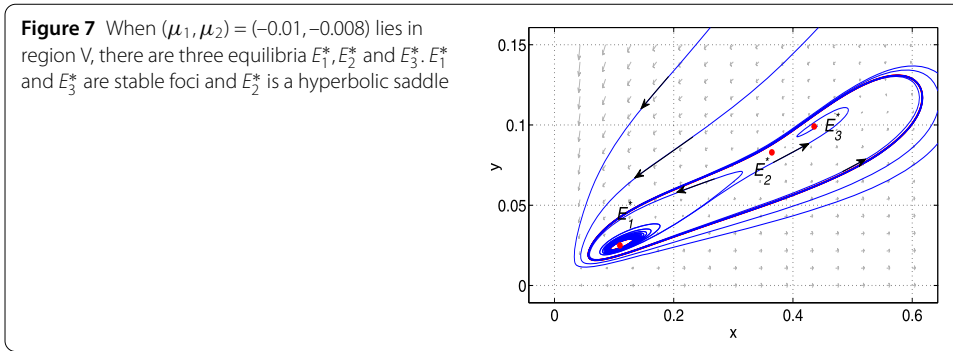


and enters into the region VI, E_1^* becomes a stable focus and an unstable limit cycle bifurcates, which indicates a subcritical Hopf bifurcation happens at E_1^* when (μ_1, μ_2) goes through H_1 . Figure 6 shows that there is a bistable state (a stable equilibrium E_1^* and a big stable limit cycle) and the unstable limit cycle bifurcated from Hopf bifurcation acts as the separatrix of attractive domains for different attractors. Eventually, trajectories can either tend to an equilibrium or a limit cycle depending on initial values of the species.

When (μ_1, μ_2) lies on the curve SN^- , a new saddle-node E^* emerges and the other equilibrium E_1^* is still a stable focus. When (μ_1, μ_2) passes through SN^- and enters into region V, there are two new equilibria E_2^* and E_3^* bifurcated from the saddle-node bifurcation. E_2^* is a hyperbolic saddle and E_3^* is a stable focus. The type of E_1^* is not changed and there is still an unstable limit cycle surrounding E_1^* . The Poincaré–Bendixson theorem implies that there is a big stable limit cycle surrounding the three equilibria and the small limit cycle, which is displayed in Fig. 7. It is shown that there is a tristable state in system (3.1). The stable and unstable manifolds of the saddle E_2^* and the unstable limit cycle act as separatrices of different attractive domains. With different initial values, the species will eventually tend to a constant state or oscillate along a big limit cycle.

When (μ_1, μ_2) lies on the curve H_1 , system (3.1) has three equilibria E_1^*, E_2^* and E_3^* , where E_1^* becomes an unstable multiple focus with multiplicity one and the types of E_2^* and E_3^* are unchanged. When (μ_1, μ_2) crosses H_1 into region IV, the unstable limit cycle enclosing E_1^* disappears and E_1^* turns into an unstable focus, which shows that system (3.1) undergoes a subcritical Hopf bifurcation when (μ_1, μ_2) passes through H_1 . The corresponding phase portrait is displayed in Fig. 8, in which E_3^* is a unique globally asymptotical attractor.

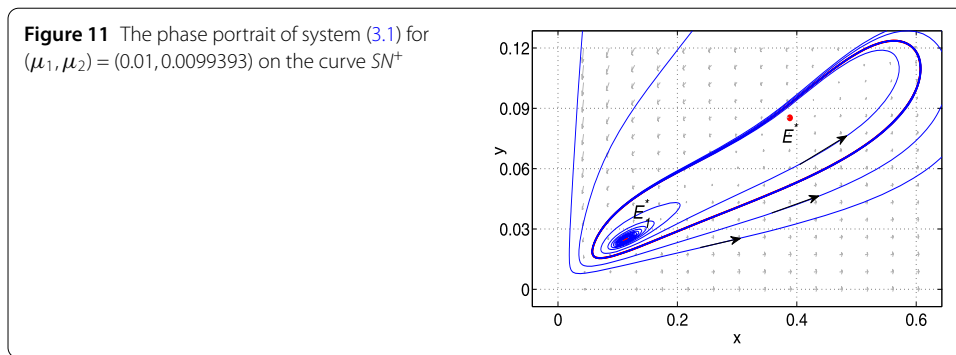
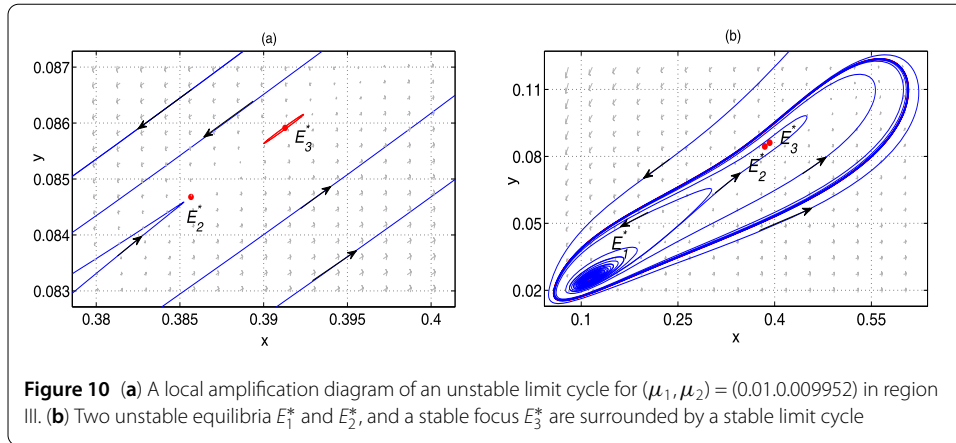
When (μ_1, μ_2) lies on the curve HL , there appears an unstable homoclinic loop to the saddle E_2^* which is displayed in Fig. 9(a), and a large stable limit cycle encloses all the equilibria and the homoclinic loop shown in Fig. 9(b). Moreover, when (μ_1, μ_2) deviates



from the curve HL , the homoclinic loop breaks, which means that system (3.1) undergoes a homoclinic bifurcation when (μ_1, μ_2) passes through the curve HL .

When (μ_1, μ_2) lies in region III, there occurs an unstable limit cycle surrounding the stable focus E_3^* , which means that system (3.1) undergoes a subcritical Hopf bifurcation when (μ_1, μ_2) passes through the curve H . For $(\mu_1, \mu_2) = (0.01, 0.009952)$, there are three equilibria, a small limit cycle and a large stable limit cycle enclosing all the equilibria and the small cycle, which is shown in Figs. 10(a) and 10(b). In this case there is also a bistable state (a stable equilibrium E_3^* and a big stable limit cycle).

When (μ_1, μ_2) goes through H and enters into region II (the region between H and SN^+), the unstable limit cycle disappears and E_3^* becomes an unstable focus while the types of E_1^* and E_2^* are not changed. When (μ_1, μ_2) lies on the curve SN^+ , two equilibria E_2^* and E_3^* overlap and become a saddle-node E^* , which means that system (3.1) undergoes a saddle-

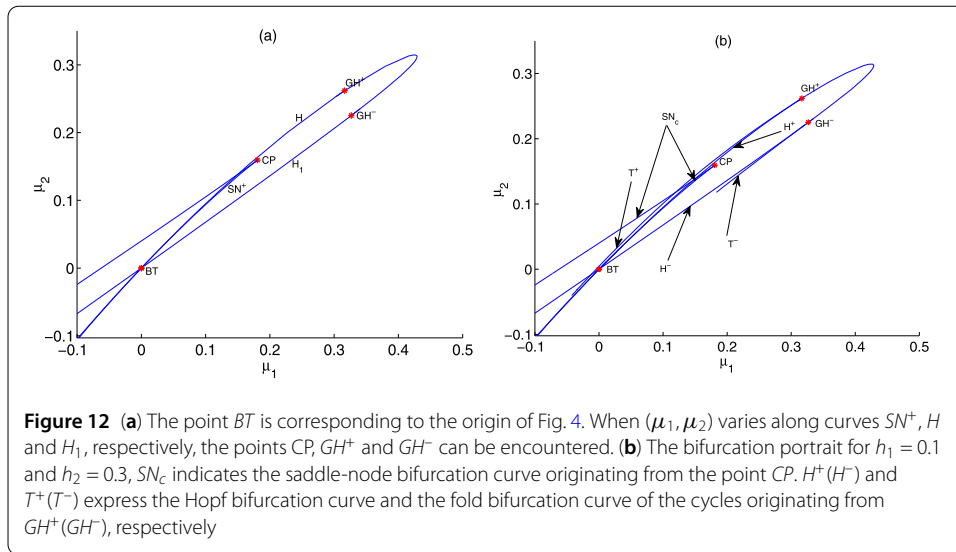


node bifurcation when (μ_1, μ_2) passes through the curve SN^+ . Whatever (μ_1, μ_2) lies in region II or on SN^+ , there both exists a stable limit cycle enclosing all the equilibria by the Poincaré–Bendixson theorem. The phase portrait of system (3.1) for (μ_1, μ_2) on the curve SN^+ is exhibited in Fig. 11. From the strategy of the optimal management of renewable resources, we find that the saddle-node bifurcation curve acts as the feasible upper bound for the rescaled harvesting efforts which guarantees the coexistence and sustainable development of the species.

From Fig. 12(a), we find that when (μ_1, μ_2) varies along the saddle-node bifurcation curve SN^+ as shown in Fig. 4, a cusp point CP can be encountered and a cusp bifurcation will happen when (μ_1, μ_2) varies near the CP point. The coordinates and parameter values for the CP point and the normal form coefficient c for the cusp bifurcation are given as follows:

$$\text{Label} = CP, (x, y, \mu_1, \mu_2) = (0.239806, 0.036775, 0.180583, 0.159373) \quad \text{and} \\ c = 7.915010.$$

When (μ_1, μ_2) varies along two Hopf bifurcation curves H and H_1 as indicated in Fig. 4, respectively, two generalized Hopf points GH^+ and GH^- can be encountered, at which both of the first Lyapunov coefficients are zero. The associated coordinates and parameter values for the two points and the second Lyapunov coefficients l_2^\pm of the generalized Hopf



bifurcations are given as follows:

$$\text{Label} = GH^+, (x, y, \mu_1, \mu_2) = (0.260349, 0.028104, 0.316434, 0.261824) \quad \text{and}$$

$$l_2^+ = -550.7068.$$

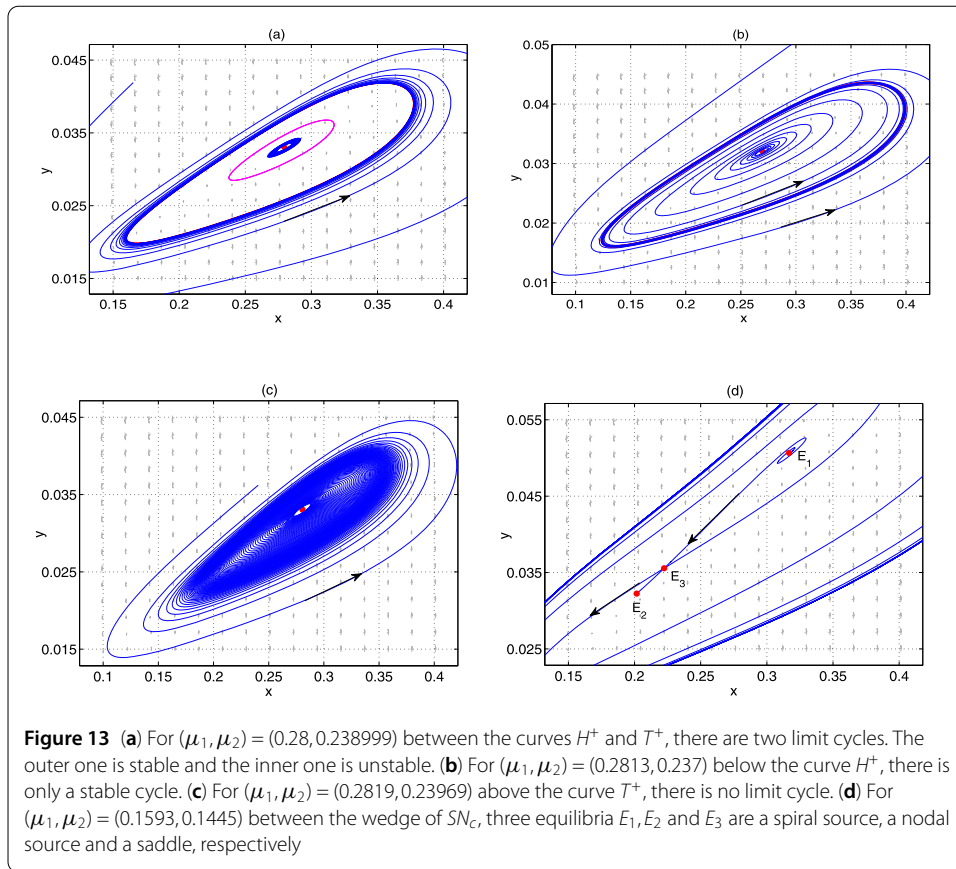
$$\text{Label} = GH^-, (x, y, \mu_1, \mu_2) = (0.126604, 0.015720, 0.326771, 0.225224) \quad \text{and}$$

$$l_2^- = -2300.709.$$

From Fig. 12(b), we find that the saddle-node bifurcation curve SN_c originating from the CP point and the saddle-node bifurcation curve SN^+ originating from the BT point are nearly coincident or tangent at the point CP . Through the curve SN_c three equilibria collide to form an equilibrium or one equilibrium splits into three equilibria. Similarly, the Hopf bifurcation curve $H (H_1)$ originating from the BT point and the Hopf bifurcation curve $H^+ (H^-)$ originating from the $GH^+ (GH^-)$ point are almost coincident and tangent at the $GH^+ (GH^-)$ point. In addition, near the Hopf bifurcation curves H^+ and H^- , two fold bifurcation curves of the cycles T^+ and T^- also appear, on which two limit cycles with different stability collide to form a semi-stable cycle. Several typical phase portraits for (μ_1, μ_2) near the generalized Hopf point GH^+ are displayed in Fig. 13. □

4 Conclusions

The prey–predator model in [20] added with constant-effort harvesting has been investigated in this paper. The Bogdanov–Takens bifurcation, the cusp bifurcation and the generalized Hopf bifurcation are discussed. By analysis, it is shown that this model can generate many novel dynamic behaviors compared with the model with no harvesting. For example, a globally asymptotically stable equilibrium can appear, while the stable equilibria in the original model are all locally asymptotically stable. Through the generalized Hopf bifurcation, the second Lyapunov coefficient can determine the relative position between the stable limit cycle and the unstable one. A cusp point CP has also been detected, from which two saddle-node bifurcation curves of equilibria emanate, through which three equilibria



collide to form an equilibrium or one equilibrium splits into three equilibria. These bifurcations have not been discussed in the original model. In addition, compared with the original model, the harvested prey–predator model can exhibit different bifurcation structure in the parameter plane. These phenomena show that the added harvesting terms play an important role in directing the evolutionary directions of the species. From the Hopf and Bogdanov–Takens bifurcations, we find that two small limit cycles bifurcating from two different equilibria are both unstable, while the big limit cycle is always stable, which shows that the ultimate numbers of the species circulate periodically along the big cycle rather than the small cycle.

Appendix

Denoting coefficients of Eq. (2.2) as $b = (h_1 - 1), c = (a + \frac{\delta - h_2}{\beta}), d = a(h_1 - 1)$ and letting $A_1 = b^2 - 3c, B = bc - 9d, C = c^2 - 3bd$, the discriminant Δ_1 of (2.2) is given by $\Delta_1 = B^2 - 4A_1C$, from which we can get $A_1 = A, \Delta_1 = \frac{A}{9}$. Suppose that x_1, x_2 and x_3 are three roots of Eq. (2.2).

$F'(x) = 3x^2 + 2(h_1 - 1)x + a + \frac{\delta - h_2}{\beta}$ and the discriminant Δ_2 of $F'(x)$ is given by $\Delta_2 = 4(h_1 - 1)^2 - 12(a + \frac{\delta - h_2}{\beta}) = 4A$. Now we prove Lemma 2.1.

- (a) If $\Delta > 0$, then $\Delta_1 > 0$. (2.2) has one real root x_1 and a pair of conjugate complex roots x_2, x_3 according to the root formula of the cubic equation. Owing to $x_1x_2x_3 = a(1 - h_1) > 0, x_1$ is the positive root of (2.2). Letting $(x^*, y^*) = (x_1, \frac{\delta - h_2}{\beta}x_1)$, now we will discuss three cases.

- (1) If $A = \frac{\Delta_2}{4} < 0$, then $F'(x^*) > 0$.
- (2) If $A = \frac{\Delta_2}{4} = 0$, then $x^* = \frac{1}{3}(1 - h_1 + \sqrt[3]{(1 - h_1)(27a - (1 - h_1)^2)})$ and $F'(x^*) = \frac{1}{3}\sqrt[3]{(1 - h_1)^2(27a - (1 - h_1)^2)^2} = \frac{1}{3}\sqrt[3]{\Delta} > 0$.
- (3) If $A = \frac{\Delta_2}{4} > 0$, then $x^* = \frac{1 - h_1 - \sqrt[3]{Y_1 - \sqrt[3]{Y_2}}}{3}$ and $F'(x^*) = \frac{1}{3}(\sqrt[3]{Y_1^2} + \sqrt[3]{Y_2^2} + 2\sqrt[3]{Y_1}\sqrt[3]{Y_2} - A) = \frac{1}{3}(\sqrt[3]{Y_1^2} + \sqrt[3]{Y_2^2} + A) > 0$, where $Y_{1,2} = (h_1 - 1)A + \frac{3(-B \pm \sqrt{\Delta_1})}{2}$.

For the above three cases, $F'(x^*) > 0$ always holds. So $E^*(x^*, y^*)$ is an anti-saddle of system (1.2).

- (b) If $\Delta = 0, A = 0$, then $x_1 = x_2 = x_3 = x^* = \frac{1 - h_1}{3}$ is a triple root of Eq. (2.2). Now system (1.2) has a unique equilibrium $E^*(x^*, y^*) = (\frac{1 - h_1}{3}, \frac{(1 - h_1)(\delta - h_2)}{3\beta})$, which is degenerated according to $F'(x^*) = 0$.
- (c) If $\Delta = 0, A > 0$, then $x_1 = 1 - h_1 + \frac{B}{A}$ and $x_2 = x_3 = -\frac{B}{2A}$ are two positive roots of Eq. (2.2) for $\max\{\frac{(h_1 - 1)^2 - 4A}{27}, 0\} < a < \frac{(h_1 - 1)^2 - A}{27}$. So system (1.2) has two equilibria:

$$\begin{aligned}
 E_1^*(x_1^*, y_1^*) &= \left(x_1, \frac{\delta - h_2}{\beta}x_1\right) \\
 &= \left(\frac{(1 - h_1)[4A + 27a - (h_1 - 1)^2]}{3A}, \frac{(\delta - h_2)(1 - h_1)[4A + 27a - (h_1 - 1)^2]}{3\beta A}\right), \\
 E^*(x^*, y^*) &= \left(x_2, \frac{\delta - h_2}{\beta}x_2\right) \\
 &= \left(\frac{(1 - h_1)[(h_1 - 1)^2 - A - 27a]}{6A}, \frac{(\delta - h_2)(1 - h_1)[(h_1 - 1)^2 - A - 27a]}{6\beta A}\right).
 \end{aligned}$$

Because of $F'(x_1^*) = \frac{1}{3A^2}[(1 - h_1)(3A + 27a - (1 - h_1)^2)]^2 = A > 0$ and $F'(x^*) = 0$, $E_1^*(x_1^*, y_1^*)$ is an anti-saddle equilibrium and $E^*(x^*, y^*)$ is a degenerated equilibrium.

- (d) If $\Delta < 0$, then $A > 0$ and (2.2) has three different roots:

$$x_1 = \frac{1 - h_1 - 2\sqrt{A} \cos \frac{\theta}{3}}{3}, \quad x_{2,3} = \frac{1 - h_1 + \sqrt{A}(\cos \frac{\theta}{3} \mp \sqrt{3} \sin \frac{\theta}{3})}{3},$$

where $\theta = \arccos T, -1 < T = \frac{2A(h_1 - 1) - 3B}{2\sqrt{A^3}} < 1$. By simple analysis, we get

$$0 < 1 - h_1 + \sqrt{A} < x_2 < 1 - h_1 + 2\sqrt{A}, \quad 0 < 1 - h_1 - \sqrt{A} < x_3 < 1 - h_1 + \sqrt{A},$$

so $x_1 > 0$. Letting

$$E_1^*(x_1^*, y_1^*) = (x_1, \frac{\delta - h_2}{\beta}x_1), E_2^*(x_2^*, y_2^*) = (x_2, \frac{\delta - h_2}{\beta}x_2), E_3^*(x_3^*, y_3^*) = (x_3, \frac{\delta - h_2}{\beta}x_3)$$

and due to

$$0 < F'(x_1^*) = \frac{4A \cos^2 \frac{\theta}{3} - A}{3} < A, \quad 0 < F'(x_3^*) = \frac{A}{9} \left(12 \cos^2 \frac{\pi - \theta}{3} - 3\right) < A,$$

$$\frac{-A}{3} < F'(x_2^*) = \frac{A}{9} \left(12 \cos^2 \frac{2\pi - \theta}{3} - 3\right) < 0,$$

hence E_1^*, E_3^* are two anti-saddle equilibria and E_2^* is a hyperbolic saddle.

Acknowledgements

The first author is supported by the Key scientific research projects of colleges and universities in Henan Province (20A110033). The second author is supported by the Basic Research Projects of Key Scientific Research Projects Plan in Henan Higher Education Institutions (20zx003), the Aeronautical Science Foundation of China (2017ZD55014), Science and Technological Research of Key Projects of Henan Province (182102210242).

Funding

No external funding.

Availability of data and materials

The authors declare that all data and material in the paper are available and veritable.

Competing interests

The authors declare that they have no competing interests.

Authors' contributions

Both authors contributed equally in writing this paper. All authors read and approved the final manuscript.

Author details

¹School of Mathematics, Zhengzhou University of Aeronautics, Zhengzhou, Henan 450046, P.R. China. ²College of Mathematics and Information Science, Henan Normal University, Xinxiang, Henan 453007, P.R. China.

Publisher's Note

Springer Nature remains neutral with regard to jurisdictional claims in published maps and institutional affiliations.

Received: 7 May 2020 Accepted: 26 March 2021 Published online: 09 April 2021

References

1. Andrews, J.F.: A mathematical model for the continuous culture of microorganisms utilizing inhibitory substrates. *Biotechnol. Bioeng.* **10**(6), 707–723 (2010)
2. Bogdanov, R.: Versal deformations of a singular point on the plane in the case of zero eigenvalues. *Funct. Anal. Appl.* **9**(2), 144–145 (1975)
3. Boon, B., Landelout, H.: Kinetics of nitrite oxidation by nitrobacter winogradski. *Biochem. J.* **85**, 440–447 (1962)
4. Chen, Q.L., Teng, Z.D., Hu, Z.Y.: Bifurcation and control for a discrete-time prey–predator model with Holling-IV functional response. *Int. J. Appl. Math. Comput. Sci.* **23**(2), 247–261 (2013)
5. Clark, C.W.: *Mathematical Bioeconomics: The Optimal Management of Renewable Resources*, 2nd edn. Wiley, New York (1990)
6. Cui, Q.Q., Zhang, Q., et al.: Complex dynamics of a discrete-time predator–prey system with Holling IV functional response. *Chaos Solitons Fractals* **87**, 158–171 (2016)
7. Dai, Y.F., Zhao, Y.L.: Hopf cyclicity and global dynamics for a predator–prey system of Leslie type with simplified Holling type IV functional response. *Int. J. Bifurc. Chaos* **28**(13), 1850166 (2018)
8. Davidowicz, P., Gliwicz, Z.M., et al.: Can Daphnia prevent a blue-green algal bloom in hypertrophic lakes? A laboratory test. *Limnologia* **19**, 21–26 (1988)
9. Edwards, V.H.: Influence of high substrate concentrations on microbial kinetics. *Biotechnol. Bioeng.* **12**(5), 679–712 (1970)
10. Gupta, R.P., Chandra, P.: Bifurcation analysis of modified Leslie–Gower predator–prey model with Michaelis–Menten type prey harvesting. *J. Math. Anal. Appl.* **398**(1), 278–295 (2013)
11. Holling, C.S.: Some characteristics of simple types of predation and parasitism. *Can. Entomol.* **91**(7), 385–398 (1959)
12. Holling, C.S.: The functional response of predator to prey density and its role in mimicry and population regulation. *Mem. Entomol. Soc. Can.* **97**, 5–60 (1965)
13. Huang, J.C., Gong, Y.J., Ruan, S.G.: Bifurcation analysis in a predator–prey model with constant-yield predator harvesting. *Discrete Contin. Dyn. Syst., Ser. B* **18**(8), 2101–2121 (2013)
14. Huang, J.C., Xia, X.J., et al.: Bifurcation of codimension 3 in a predator–prey system of Leslie type with simplified Holling type IV functional response. *Int. J. Bifurc. Chaos* **26**(2), 1650034 (2016)
15. Huang, J.C., Xiao, D.M.: Analyses of bifurcations and stability in a predator–prey system with Holling type-IV functional response. *Acta Math. Appl. Sin. Engl. Ser.* **20**(1), 167–178 (2004)
16. Huang, M.Z., Liu, S.Z., et al.: Periodic solutions and homoclinic bifurcation of a predator–prey system with two types of harvesting. *Nonlinear Dyn.* **73**(1–2), 815–826 (2013)
17. Kar, T.K., Ghorai, A.: Dynamic behaviour of a delayed predator–prey model with harvesting. *Appl. Math. Comput.* **217**(22), 9085–9104 (2011)
18. Kar, T.K., Matsuda, H.: Global dynamics and controllability of a harvested prey–predator system with Holling type III functional response. *Nonlinear Anal. Hybrid Syst.* **1**(1), 59–67 (2007)
19. Leslie, P.H., Gower, J.C.: The properties of a stochastic model for the predator–prey type of interaction between two species. *Biometrika* **47**, 219–234 (1960)
20. Li, Y.L., Xiao, D.M.: Bifurcations of a predator–prey system of Holling and Leslie types. *Chaos Solitons Fractals* **34**(2), 606–620 (2007)
21. Liu, M., Hu, D.P., Meng, F.W.: Stability and bifurcation analysis in a delay-induced predator–prey model with Michaelis–Menten type predator harvesting. *Discrete Contin. Dyn. Syst., Ser. S* (2020). <https://doi.org/10.3934/dcdss.2020259>
22. Makinde, O.D.: Solving ratio-dependent predator–prey system with constant effort harvesting using Adomian decomposition method. *Appl. Math. Comput.* **186**(1), 17–22 (2007)

23. Perko, L.: *Differential Equations and Dynamical Systems*. Springer, New York (1996)
24. Sen, M., Banerjee, M., Morozov, A.: Bifurcation analysis of a ratio-dependent prey–predator model with the Allee effect. *Ecol. Complex.* **11**, 12–27 (2012)
25. Sokol, W., Howell, J.A.: Kinetics of phenol oxidation by washed cell. *Biotechnol. Bioeng.* **23**(9), 2039–2049 (1981)
26. Solomon, M.E.: The natural control of animal populations. *J. Anim. Ecol.* **19**, 1–35 (1949)
27. Takens, F.: Forced oscillations and bifurcation. *Applications of global analysis I. Comm. Math. Inst.* **3**, 1–62 (2001)
28. Tener, J.S.: *Muskoxen*. Queens Printer, Ottawa (1965)
29. Xiao, D.M., Jennings, L.S.: Bifurcations of a ratio-dependent predator–prey system with constant rate harvesting. *SIAM J. Appl. Math.* **65**(3), 737–753 (2005)
30. Xiong, Z.L., Xue, Y., Li, S.Y.: A food chain system with Holling IV functional responses and impulsive effect. *Int. J. Biomath.* **1**(3), 361–375 (2008)
31. Yang, R.D., Humphrey, A.E.: Dynamics and steady state studies of phenol biodegeneration in pure and mixed cultures. *Biotechnol. Bioeng.* **17**, 1211–1235 (1975)
32. Zhang, S.W., Wang, F.Y., Chen, L.S.: A food chain model with impulsive perturbations and Holling IV functional response. *Chaos Solitons Fractals* **26**(3), 855–866 (2005)
33. Zhu, C.R., Lan, K.Q.: Phase portraits, Hopf bifurcations and limit cycles of Leslie–Gower predator–prey systems with harvesting rates. *Discrete Contin. Dyn. Syst., Ser. B* **14**(1), 289–306 (2010)
34. Zhu, Q., Peng, H.Q., et al.: Bifurcation analysis of a stage-structured predator–prey model with prey refuge. *Discrete Contin. Dyn. Syst., Ser. S* **12**(7), 2195–2209 (2019)

Submit your manuscript to a SpringerOpen[®] journal and benefit from:

- Convenient online submission
- Rigorous peer review
- Open access: articles freely available online
- High visibility within the field
- Retaining the copyright to your article

Submit your next manuscript at ► [springeropen.com](https://www.springeropen.com)
